Available online at www.sciencedirect.com
ScienceDirect
Solar Energy 82 (2008) 354–367
SOLAR ENERGY
www.elsevier.com/locate/solener

Optimal sizing method for stand-alone hybrid solar–wind system with LPSP technology by using genetic algorithm

Hongxing Yang [a,*], Wei Zhou [a], Lin Lu [a], Zhaohong Fang [b]

[a] Department of Building Services Engineering, The Hong Kong Polytechnic University, Hung Hom, Kowloon, Hong Kong
[b] School of Thermal Engineering, Shangdong University of Architecture, Jinan, Shandong, China

Received 12 March 2007; received in revised form 7 August 2007; accepted 14 August 2007
Available online 19 September 2007

Communicated by: Associate Editor M. Patel

Abstract

System power reliability under varying weather conditions and the corresponding system cost are the two main concerns for designing hybrid solar–wind power generation systems. This paper recommends an optimal sizing method to optimize the configurations of a hybrid solar–wind system employing battery banks. Based on a genetic algorithm (GA), which has the ability to attain the global optimum with relative computational simplicity, one optimal sizing method was developed to calculate the optimum system configuration that can achieve the customers required loss of power supply probability (LPSP) with a minimum annualized cost of system (ACS). The decision variables included in the optimization process are the PV module number, wind turbine number, battery number, PV module slope angle and wind turbine installation height. The proposed method has been applied to the analysis of a hybrid system which supplies power for a telecommunication relay station, and good optimization performance has been found. Furthermore, the relationships between system power reliability and system configurations were also given.

Keywords: Hybrid solar–wind system; Optimization; LPSP; Annualized cost of system; Genetic algorithm

1. Introduction

The rapid depletion of fossil fuel resources on a worldwide basis has necessitated an urgent search for alternative energy sources to cater to the present day demands. Alternative energy resources such as solar and wind have attracted energy sectors to generate power on a large scale. A drawback, common to wind and solar options, is their unpredictable nature and dependence on weather and climatic changes, and the variations of solar and wind energy may not match with the time distribution of demand.

Fortunately, the problems caused by the variable nature of these resources can be partially overcome by integrating the two resources in proper combination, using the strengths of one source to overcome the weakness of the other. The hybrid systems that combine solar and wind generating units with battery backup can attenuate their individual fluctuations and reduce energy storage requirements significantly. However, some problems stem from the increased complexity of the system in comparison with single energy systems. This complexity, brought about by the use of two different resources combined, makes an analysis of hybrid systems more difficult.

In order to efficiently and economically utilize the renewable energy resources, one optimum match design sizing method is necessary. The sizing optimization method can help to guarantee the lowest investment with adequate and full use of the solar system, wind system and battery bank, so that the hybrid system can work at optimum

* Corresponding author. Tel.: +852 2766 5863; fax: +852 2774 6146.
E-mail address: behxyang@polyu.edu.hk (H. Yang).

0038-092X/$ - see front matter © 2007 Elsevier Ltd. All rights reserved.
doi:10.1016/j.solener.2007.08.005

Nomenclature

ACS	annualized cost of system, US$
CRF	the capital recovery factor
EFC	equivalent full cycles of the battery
f	annual inflation rate
G	solar radiation, W/m^2
H	height, m
h	heat transfer coefficient, W/m^2 °C
I	current, A
i and i'	the real and nominal interest rate
LPSP	loss of power supply probability
n	ideality factor
P	power, W
Q	heat transfer amount, W
R	resistance, ohm
SFF	the sinking fund factor
SOC	battery state of charge
T	temperature, K
t	time, h
V	voltage, V
v	velocity, m/s
Y	lifetime, year

Greeks

α, β, γ	constant parameters for PV module
α'	absorptivity
β'	PV module slope angle, radians
ε	emissivity
η	charging and discharging efficiency
ζ	wind speed power law coefficient
σ	hourly self-discharge rate

Subscripts

acap	annualized capital cost
amin	annualized maintenance cost
arep	annualized replacement cost
bat	battery
bh	beam radiation on horizontal surface
bt	beam radiation on tilt surface
cap	initial capital cost
dt	diffuse radiation on tilt surface
O	parameters under standard conditions
OC	open-circuit
P	parallel
proj	project
PV	photovoltaic
r	reference
re	reflected
rep	replacement
s	series
SC	short-circuit
tt	total radiation on tilt surface
WT	wind turbine

conditions in terms of investment and system power reliability requirement.

Various optimization techniques such as the probabilistic approach, graphical construction method and iterative technique have been recommended by researchers.

Tina et al. (2006) presented a probabilistic approach based on the convolution technique to incorporate the fluctuating nature of the resources and the load, thus eliminating the need for time-series data, to assess the long-term performance of a hybrid solar–wind system for both stand-alone and grid-connected applications.

A graphical construction technique for figuring the optimum combination of battery and PV array in a hybrid solar–wind system has been presented by Borowy and Salameh (1996). The system operation is simulated for various combinations of PV array and battery sizes and the loss of power supply probability (LPSP). Then, for the desired LPSP, the PV array versus battery size is plotted and the optimal solution, which minimizes the total system cost, can be chosen. Another graphical technique has been given by Markvart (1996) to optimize the size of a hybrid solar–wind energy system by considering the monthly average solar and wind energy values. However, in both graphical methods, only two parameters (either PV and battery, or PV and wind turbine) were included in the optimization process.

Yang et al. (2003, 2007) have proposed an iterative optimization technique following the loss of power supply probability (LPSP) model for a hybrid solar–wind system. The number selection of the PV module, wind turbine and battery ensures the load demand according to the power reliability requirement, and the system cost is minimized. Similarly, an iterative optimization method was presented by Kellogg et al. (1998) to select the wind turbine size and PV module number needed to make the difference of generated and demanded power (DP) as close to zero as possible over a period of time. From this iterative procedure, several possible combinations of solar–wind generation capacities were obtained. The total annual cost for each configuration is then calculated and the combination with the lowest cost is selected to represent the optimal mixture.

Eftichios Koutroulis et al. (2006) proposed a methodology for optimal sizing of stand-alone PV/WG systems. The purpose of the proposed methodology is to suggest, among a list of commercially available system devices, the optimal number and type of units ensuring that the 20-year round total system cost is minimized subject to the constraint that the load energy requirements are completely covered,

resulting in zero load rejection. This methodology can find the global optimum system configuration with relative computational simplicity, but the configurations are sometimes not cost effective, because sometimes a tiny amount of load rejections are tolerable to the customers in order to gain an acceptable system cost.

A common disadvantage of the optimization methods described above is that they still have not found the best compromise point between system power reliability and system cost. The minimization of system cost function is normally implemented by employing probability programming techniques or by linearly changing the values of corresponding decision variables, resulting in suboptimal solutions and sometimes increased computational effort requirements. Also, these sizing methodologies normally do not take into account some system design characteristics, such as PV modules slope angle and wind turbine installation height, which also highly affect the resulting energy production and system installation costs.

In this paper, one optimal sizing model for a stand-alone hybrid solar–wind system employing battery banks is developed based on the loss of power supply probability (LPSP) and the annualized cost of system (ACS) concepts. The optimization procedure aims to find the configuration that yields the best compromise between the two considered objectives: LPSP and ACS. The decision variables included in the optimization process are the PV module number, wind turbine number, battery number, and also the PV module slope angle as well as the wind turbine installation height. The configurations of a hybrid system that can meet the system power reliability requirements with minimum cost can be obtained by an optimization technique – the genetic algorithm (GA), which is an advanced search and optimization technique; it is generally robust in finding global optimal solutions, particularly in multi-modal and multi-objective optimization problems, where the location of the global optimum is a difficult task.

2. Model of the hybrid system components

A hybrid solar–wind power generation system consists of PV array, wind turbine, battery bank, inverter, controller, and other accessory devices and cables. A schematic diagram of the basic hybrid system is shown in Fig. 1. The PV array and wind turbine work together to satisfy the load demand. When energy sources (solar and wind energy) are abundant, the generated power, after satisfying the load demand, will be supplied to feed the battery until it is full charged. On the contrary, when energy sources are poor, the battery will release energy to assist the PV array and wind turbine to cover the load requirements until the storage is depleted.

In order to predict the hybrid system performance, individual components need to be modeled first and then their mix can be evaluated to meet the load demand.

2.1. PV system model

The power generation simulation model for the PV system is composed of three parts: PV array power model, solar radiation on PV module surface and PV module temperature model.

2.1.1. PV array power model

PV module performance is highly influenced by weather conditions, especially solar radiation and PV module temperature. A simplified simulation model (Zhou et al., 2007) with acceptable precision is used to estimate the actual performance of PV modules under varying operating conditions. Five parameters (α, β, γ, R_s and n_{MPP}) are introduced to take account for all the nonlinear effects of the environmental factors on PV module performance. Using the definition of fill factor, the maximum power output delivered by the PV module can be written as

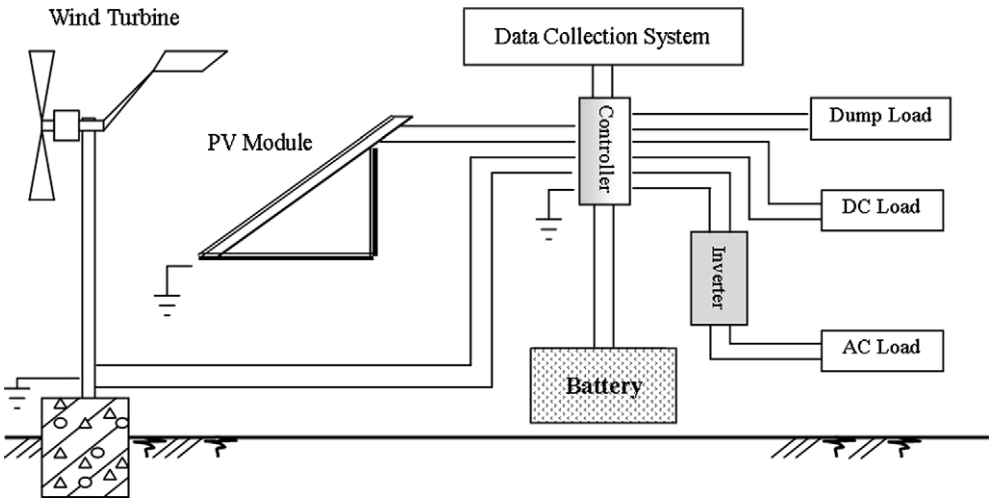

Fig. 1. Block diagram of the hybrid solar–wind system.

$$P_{\text{module}} = \frac{\frac{V_{\text{oc}}}{n_{\text{MPP}}KT/q} - \ln\left(\frac{V_{\text{oc}}}{n_{\text{MPP}}KT/q} + 0.72\right)}{1 + \frac{V_{\text{oc}}}{n_{\text{MPP}}KT/q}} \cdot \left(1 - \frac{R_{\text{s}}}{V_{\text{oc}}/I_{\text{sc}}}\right) \cdot I_{\text{sco}} \left(\frac{G}{G_0}\right)^{\alpha} \cdot \frac{V_{\text{oco}}}{1 + \beta \ln \frac{G_0}{G}} \cdot \left(\frac{T_0}{T}\right)^{\gamma} \quad (1)$$

where n_{MPP} is the ideality factor at the maximum power point ($1 < n_{\text{MPP}} < 2$), because the PV systems are usually equipped with a maximum power point tracker to maximize power output, it is reasonable to believe that the PV module working states will stay around the maximum power point. Therefore, n_{MPP} is used to present the ideality factor of the PV module. K is the Boltzmann constant (1.38×10^{-23} J/K); T is the PV module temperature, K; q is the magnitude of the electron charge (1.6×10^{-19} C); R_{s} is the series resistance, ohm; α is the factor responsible for all the nonlinear effects that the photocurrent depends on; β is a PV module technology specific-related dimensionless coefficient (Van Dyk et al., 2002); and γ is the factor considering all the nonlinear temperature–voltage effects.

In order to calculate the five parameters, only limited data are needed. The detailed data used for the parameter evaluation are listed in Table 1, they are the short-circuit-current I_{sc}, open-circuit-voltage V_{oc}, maximum power point current I_{MPP} and voltage V_{MPP} of the PV module under two different solar irradiance intensities (G_0, G_1) and two PV module temperatures (T_0, T_1). These data are normally available from the manufactures, and the regression results for the PV module used in this study are given in Table 2. Then the simulation model can be used for PV module performance predictions.

PV modules represent the fundamental power conversion unit of a PV system, if a matrix of $N_{\text{s}} \times N_{\text{p}}$ PV modules is considered, the maximum power output of the PV system can be calculated by

$$P_{\text{PV}} = N_{\text{p}} \cdot N_{\text{s}} \cdot P_{\text{module}} \cdot \eta_{\text{MPPT}} \cdot \eta_{\text{oth}} \quad (2)$$

where η_{MPPT} is efficiency of the maximum power point tracking, although it is variable according to different working conditions, a constant value of 95% is assumed to simplify the calculations. η_{oth} is the factor representing the other losses such as the loss caused by cable resistance, accumulative dust, etc.

Thus, once the solar radiation on the module surface and the PV module temperature are known, the power output of the PV system can be predicted.

Table 1
Detailed data requirements for parameter estimation

	G_0	G_1
T_0	I_{sc}, V_{oc}, I_{MPP}, V_{MPP}	I_{sc}, V_{oc}, I_{MPP}, V_{MPP}
T_1	Null	V_{oc}

Table 2
Parameter estimation results for the PV module performance

	α	β	γ	n_{MPP}	R_{s} (Ω)
Item	1.21	0.058	1.15	1.17	0.012

2.1.2. Solar radiation on PV module surface

The PV module can be placed at any orientation and at any slope angle, but most local observatories only provide solar radiation data on a horizontal plane. Thus, an estimate of the total solar radiation incident on the PV module surface is needed. Generally, the total solar radiation on a tilted surface is calculated by adding the beam, diffuse and reflected solar radiation components on the tilted surface:

$$G_{\text{tt}} = G_{\text{bt}} + G_{\text{dt}} + G_{\text{re}} \quad (3)$$

where G_{tt} is the total solar radiation on a tilt surface; G_{bt}, G_{dt} and G_{re} are the beam, diffuse and reflected radiation on the tilt surface. The reflected part is neglected in the following calculations.

(a) Beam radiation
The beam part can be simulated by the following formula:

$$G_{\text{bt}} = G_{\text{bh}} \cdot \frac{\cos\theta}{\cos\theta_z} \quad (4)$$

where θ is the angle of incidence, which can be calculated by (Duffie and Beckman, 1980)

$$\cos\theta = \sin\delta\sin\phi\cos\beta' - \sin\delta\cos\phi\sin\beta'\cos\gamma' + \cos\delta\cos\phi\cos\beta'\cos\omega + \cos\delta\sin\phi\sin\beta' \times \cos\gamma'\cos\omega + \cos\delta\sin\beta'\sin\gamma'\sin\omega \quad (5)$$

And θ_z is the angle of incidence for horizontal surfaces:

$$\cos\theta_z = \cos\delta\cos\phi\cos\omega + \sin\delta\sin\phi \quad (6)$$

where δ is the solar declination, $-23.45° \leqslant \delta \leqslant 23.45°$; ϕ is the latitude of local location; β' is the slope angle of the PV module; γ' is the surface azimuth angle; and ω is the hour angle.

(b) Diffuse radiation
The Perez model (Perez et al., 1990) is utilized to estimate the diffuse radiation on the module surface. This model accounts for circumsolar, horizon brightening, and isotropic diffuse radiation by empirically derived "reduced brightness coefficients". Then, the solar diffuse radiation on the titled surface can be estimated by

$$G_{\text{dt}} = G_{\text{dh}} \cdot \cos^2\left(\frac{\beta'}{2}\right) \cdot (1 - F_1) + G_{\text{dh}} \cdot F_1 \cdot \left(\frac{a}{c}\right) + G_{\text{dh}} \cdot F_2 \cdot \sin\beta' \quad (7)$$

The brightness coefficients F_1 and F_2, are functions of sky clearness ε, and sky brightness parameter.

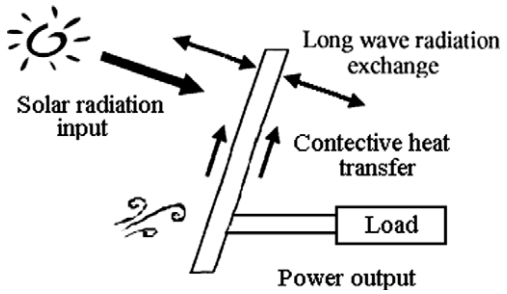

Fig. 2. Heat transfer diagram of the PV module.

2.1.3. PV module temperature model

Operating temperature has a strong effect on the electrical response of PV modules (Luis and Sivestre, 2002). Most local observatories only provide surrounding air temperature, thus, an estimate of the PV module temperature is needed. The module temperature is estimated in this paper by considering the thermal energy exchange of the module with its environment through the main heat transfer paths. The convection and radiation heat transfer from the front and back surfaces (see Fig. 2) of the module are considered significant, whilst the heat conducted from the array to the structural framework and the building is considered negligible due to the small area of contact points.

2.1.3.1. Solar radiation input. The effective solar energy reaching the front surface of the module is a function of the short wave solar radiation inputs and the absorptivity of the module surface

$$Q_G = \alpha' \cdot A \cdot G \tag{8}$$

The absorptivity α' is a function of the configuration and material of the solar module. A constant α' of 77%, a proper energy range to be absorbed by the PV module, is assumed in the following analysis.

2.1.3.2. Long wave radiation heat transfer. The long wave radiation of a body at temperature T is given by the Stefan–Boltzmann law. Then the total long wave energy exchange between the PV module and surrounding space (the sky and the ground) is

$$Q_{\text{radia}} = \alpha' \cdot A \cdot \sigma \cdot (\varepsilon_{\text{sky}} \cdot T_{\text{sky}}^4 + \varepsilon_{\text{ground}} \cdot T_{\text{ground}}^4 - 2 \cdot \varepsilon_{\text{PV}} \cdot T_{\text{PV}}^4) \tag{9}$$

2.1.3.3. Convective heat transfer. The convection may be a combination of free and forced convection effects. For the free convection effects, an approximation given by Holman (1992) is used. For forced cooling, it is approximated as a linear function of wind speed. Then, the total convective energy exchange for the PV module is

$$\begin{aligned} Q_{\text{conoutput}} &= h_{\text{c,free}} + h_{\text{c,forced}} \\ &= 2A \cdot [1.31 \cdot (T_{\text{PV}} - T_{\text{air}})^{1/3} + 0.5 \cdot v_{\text{wind}}] \\ &\quad \cdot (T_{\text{PV}} - T_{\text{air}}) \end{aligned} \tag{10}$$

2.1.3.4. PV module temperature. Therefore, the PV module's steady state temperature can be calculated by the following energy balance:

$$\begin{aligned} &\alpha' \cdot A \cdot [G + \sigma \cdot (\varepsilon_{\text{sky}} \cdot T_{\text{sky}}^4 + \varepsilon_{\text{ground}} \cdot T_{\text{ground}}^4 - 2 \cdot \varepsilon_{\text{PV}} \cdot T_{\text{PV}}^4)] \\ &\quad = 2A \cdot [1.31 \cdot (T_{\text{PV}} - T_{\text{air}})^{1/3} + 0.5 \cdot v_{\text{wind}}] \cdot (T_{\text{PV}} - T_{\text{air}}) \\ &\quad\quad + P_{\text{module}} \end{aligned} \tag{11}$$

Some parameters can be found from Schott (1985): $\varepsilon_{\text{sky}} = 0.95$ for clear conditions; $\varepsilon_{\text{sky}} = 1.0$ for overcast conditions, $\varepsilon_{\text{ground}} = 0.95$, $\varepsilon_{\text{PV}} = 0.8$, $T_{\text{sky}} = T_{\text{air}} - 20$ for clear sky conditions, $T_{\text{sky}} = T_{\text{air}}$ for overcast conditions.

2.2. Wind turbine system model

Choosing a suitable model is very important for wind turbine power simulations. There are three main factors that determine the power output of a wind turbine, i.e. the power output curve (determined by aerodynamic power efficiency, mechanical transmission η_{m} and converting electricity efficiency η_{g}) of a chosen wind turbine, the wind speed distribution of a selected site where the wind turbine is installed, and the tower height.

The power curve of a wind turbine is nonlinear, the data is available from the manufacturer, and can be easily digitized and the resulting table can be used to simulate the wind turbine performance.

Wind speed changes with height and the available wind data at different sites are normally measured at different height levels. The wind power law has been recognized as a useful tool to transfer the anemometer data recorded at certain levels to the desired hub center:

$$v = v_{\text{r}} \left(\frac{H_{\text{WT}}}{H_{\text{r}}} \right)^{\xi} \tag{12}$$

where v is the wind speed at the wind turbine height H_{WT}, m/s; v_{r} is the wind speed measured at the reference height H_{r}, m/s; and the parameter ζ is the wind speed power law coefficient. The value of the coefficient varies from less than 0.10 for very flat land, water or ice to more than 0.25 for heavily forested landscapes. The one-seventh power law (0.14) is a good reference number for relatively flat surfaces such as the open terrain of grasslands away from tall trees or buildings (Gipe, 1995).

2.3. Battery model

The battery bank, which is usually of the lead-acid type, is used to store surplus electrical energy, to regulate system voltage and to supply power to load in case of low wind speed and/or low solar conditions. Lead-acid batteries used in hybrid solar–wind systems operate under very specific conditions, and it is often very difficult to predict when energy will be extracted from or supplied to the battery. Here in this paper, several factors that affect the battery behaviors have been taken into account, such as the

charging current rate, the charging efficiency, the self-discharge rate as well as the battery capacity.

Most battery models mainly focus on three different characteristics, i.e. the battery state of charge (SOC) as well as the floating charge voltage (or the terminal voltage) and the battery lifetime.

2.3.1. Battery state-of-charge (SOC)

Energy will be stored in the batteries when the power generated by the wind turbine and PV array is greater than the load. When power generation cannot satisfy the load requirements, energy will be extracted from the batteries, and the load will be cut off when power generation by both wind turbine and PV array is insufficient and the storage is depleted.

Like all chemical processes, the battery capacity is temperature dependent. Generally, the battery capacity changes can be expressed by using the temperature coefficient δ_C (Berndt, 1994):

$$C'_{bat} = C''_{bat} \cdot (1 + \delta_C \cdot (T_{bat} - 298.15)) \tag{13}$$

where C'_{bat} is the available or practical capacity of the battery when the battery temperature is T_{bat}, Ah; C''_{bat} is the nominal or rated capacity of the battery, which is the value of the capacity given by the manufacturer as the standard value that characterizes this battery, Ah; a temperature coefficient of $\delta_C = 0.6\%$ per degree, is usually used unless otherwise specified by the manufacturer (Berndt, 1994).

For perfect knowledge of the real SOC of a battery, it is necessary to know the initial SOC, the charge or discharge time and the current. However, most storage systems are not ideal, losses occur during charging and discharging and also during storage periods. Taking these factors into account, the SOC of the battery at time $t+1$ can be simply calculated by

$$\mathrm{SOC}(t+1) = \mathrm{SOC}(t) \cdot \left(1 - \frac{\sigma \cdot \Delta t}{24}\right) + \frac{I_{bat}(t) \cdot \Delta t \cdot \eta_{bat}}{C'_{bat}} \tag{14}$$

where σ is the self-discharge rate which depends on the accumulated charge and the battery state of health (Guasch and Silvestre, 2003), and a proposed value of 0.2% per day is recommended. It is difficult to measure separate charging and discharging efficiencies, so manufacturers usually specify a round-trip efficiency. In this paper, the battery charge efficiency is set equal to the round-trip efficiency, and the discharge efficiency is 1.

The current rate of the battery at time t for the hybrid solar–wind system can be described by

$$I_{bat}(t) = \frac{P_{PV}(t) + P_{WT}(t) - P_{AC\ load}(t)/\eta_{inverter} - P_{DC\ load}(t)}{V_{bat}(t)} \tag{15}$$

The inverter efficiency $\eta_{inverter}$ is considered to be 92% according to the load profile and the specifications of the inverter. In this case, the wind turbine is assumed to have DC output, so the use of a rectifier is not necessary. But if the wind turbine is designed to connect to an AC grid, then the rectifier losses should be considered for the part of wind energy that has been rectified from AC to DC.

2.3.2. Battery floating charge voltage

The battery floating charge voltage response under both charging and discharging conditions is modeled by the equation-fit method, which treats the battery as a black box and expresses the battery floating charge voltage by a polynomial in terms of battery SOC and battery current

$$V'_{bat} = A \times (\mathrm{SOC})^3 + B \times (\mathrm{SOC})^2 + C \times \mathrm{SOC} + D \tag{16}$$

where V'_{bat} is the battery floating charge voltage, in order to take into account the temperature effect on battery voltage predictions, the temperature coefficient δ_V is applied (Berndt, 1994)

$$V_{bat} = V'_{bat} + \delta_V \cdot (T_{bat} - 298.15) \tag{17}$$

where V_{bat} is the calibrated voltage of the battery, after the temperature effects have been considered. The temperature coefficient δ_V is assumed to be a constant of -4 mV/°C per 2 V cell for the considered battery temperature range in this research.

Parameters A, B, C and D in Eq. (16) are functions of the battery current I, and can be calculated by the following second degree polynomial equations:

$$\begin{pmatrix} A \\ B \\ C \\ D \end{pmatrix} = \begin{pmatrix} a_1 & a_2 & a_3 \\ b_1 & b_2 & b_3 \\ c_1 & c_2 & c_3 \\ d_1 & d_2 & d_3 \end{pmatrix} \begin{pmatrix} I^2 \\ I \\ 1 \end{pmatrix} \tag{18}$$

The parameters $a_1, a_2, a_3, \ldots, d_1, d_2, d_3$ can be determined using the least squares fitting method by fitting the equations to battery performance data (usually available from the manufacturer). The parameters for the battery used in the following project analysis are calculated to be:

$$\begin{pmatrix} a_1 & a_2 & a_3 \\ b_1 & b_2 & b_3 \\ c_1 & c_2 & c_3 \\ d_1 & d_2 & d_3 \end{pmatrix} = \begin{cases} \begin{pmatrix} -0.00152 & 0.05509 & 0.15782 \\ 0.00165 & -0.05758 & -0.39049 \\ -0.00024 & 0.01018 & 0.52391 \\ -0.00014 & 0.00795 & 1.86557 \end{pmatrix} & I > 0 \\ \begin{pmatrix} 0.00130 & 0.00093 & 0.03533 \\ -0.00201 & -0.00803 & -0.08716 \\ 0.00097 & 0.00892 & 0.22999 \\ -0.00021 & -0.00306 & 1.93286 \end{pmatrix} & I < 0 \end{cases} \tag{19}$$

where $I > 0$ represents the battery charging process, and $I < 0$ for the discharging process. Once these parameters are estimated, the battery model can be used for the simulations.

2.3.3. Battery lifetime

Two independent limitations on the lifetime of battery banks (the battery cycle life $Y_{bat,c}$ and the battery float life $Y_{bat,f}$) are employed.

Battery cycle life $Y_{bat,c}$ is the length of time that the battery will last under normal cycles before it requires replacement; it depends on the depth of discharge of individual cycles. During the battery lifetime, a great number of individual cycles may occur, including the charging and discharging process, and every discharging process will result in some depletion of the battery. Here the equivalent full cycles (EFC) concept (Ashari and Nayar, 1999) has been taken, an average EFC will be given, and after all the equivalent cycles, the battery will need to be replaced.

The battery float life $Y_{bat,f}$ is the maximum length of time that the battery will last before it needs replacement, regardless of how much or how little it is used. This limitation is typically associated with the damage caused by corrosion in the battery, which is strongly affected by temperature. Higher ambient temperatures are more conducive to corrosion, so a battery installed in warm surroundings would have a shorter float life than one installed in air-conditioned surroundings.

Considering these two lifetime aspects or limitations, the battery will be exhausted either from use or from old age, depending on which one is shorter.

2.3.4. Battery simulation constraints

The battery SOC was used as a decision variable for the control of battery overcharge and discharge protections. The case of overcharge may occur when higher power is generated by the PV array and wind turbine, or when low load demand exists. In such a case when the battery SOC reaches the maximum value, $SOC_{max} = 1$, the control system intervenes and stops the charging process. On the other hand, if the state of charge decreases to a minimum level, $SOC_{min} = 1 - DOD$, the control system disconnects the load. This is important to prevent against batteries shortening their lifetime or even their destruction. Also, for longevity of battery life, the maximum charging rate, SOC/5, is given as the upper limit.

3. Power reliability model based on LPSP concept

Because of the intermittent solar radiation and wind speed characteristics, which highly influence the resulting energy production, power reliability analysis has been considered as an important step in any system design process. A reliable electrical power system means a system has sufficient power to feed the load demand during a certain period or, in other words, has a small loss of power supply probability (LPSP). LPSP is defined as the probability that an insufficient power supply results when the hybrid system (PV array, wind turbine and battery storage) is unable to satisfy the load demand (Yang et al., 2003). It is a feasible measure of the system performance for an assumed or known load distribution. A LPSP of 0 means the load will always be satisfied; and an LPSP of 1 means that the load will never be satisfied. Loss of power supply probability (LPSP) is a statistical parameter; its calculation is not only focused on the abundant or bad resource period. Therefore, in a bad resource year, the system will suffer from a higher probability of losing power.

There are two approaches for the application of LPSP in designing a stand-alone hybrid system. The first one is based on chronological simulation. This approach is computationally burdensome and requires the availability of data spanning a certain period of time. The second approach uses probabilistic techniques to incorporate the fluctuating nature of the resource and the load, thus eliminating the need for time-series data. Considering the energy accumulation effect of the battery, to present the system working conditions more precisely, the chronological method is employed in this research. The objective function, LPSP, from time 0 to T can then be described by

$$\begin{aligned} \mathrm{LPSP} &= \frac{\sum_{t=0}^{T} \mathrm{Power} \cdot \mathrm{failure} \cdot \mathrm{time}}{T} \\ &= \frac{\sum_{t=0}^{T} \mathrm{Time}(P_{\mathrm{available}}(t) < P_{\mathrm{needed}}(t))}{T} \end{aligned} \tag{20}$$

where T is the number of hours in this study with hourly weather data input. The power failure time is defined as the time that the load is not satisfied when the power generated by both the wind turbine and the PV array is insufficient and the storage is depleted (battery SOC falls below the allowed value $SOC_{min} = 1 - DOD$ and still has not recovered to the reconnection point). The power needed by the load side can be expressed as

$$P_{\mathrm{needed}}(t) = \frac{P_{\mathrm{AC\ load}}(t)}{\eta_{\mathrm{inverter}}(t)} + P_{\mathrm{DC\ load}}(t) \tag{21}$$

and the power available from the hybrid system is expressed by

$$\begin{aligned} P_{\mathrm{available}}(t) = P_{\mathrm{PV}} + P_{\mathrm{WT}} + C \cdot V_{\mathrm{bat}} \\ \cdot \mathrm{Min}\left[I_{\mathrm{bat,max}} = \frac{0.2C'_{\mathrm{bat}}}{\Delta t}, \frac{C'_{\mathrm{bat}} \cdot (\mathrm{SOC}(t) - \mathrm{SOC}_{\mathrm{min}})}{\Delta t} \right] \end{aligned} \tag{22}$$

where C is a constant, 0 for battery charging process and 1 for battery discharging process. SOC(t) is the battery state-of-charge at time t, and it is calculated based on the battery SOC at the previous time $t - 1$ by using Eq. (14). The wind turbine, as mentioned before, is assumed to have DC output, so the rectifier is not used. But if the wind turbine is designed to have AC output, then the rectifier losses should be considered for the part of wind energy that has been rectified from AC to DC.

Using the above developed objective function according to the LPSP technique, for a given LPSP value for one year, a set of system configurations, which satisfy the system power reliability requirements, can be obtained.

4. Economic model based on ACS concept

The optimum combination of a hybrid solar–wind system can make the best compromise between the two considered objectives: the system power reliability and system cost. The economical approach, according to the concept of annualized cost of system (ACS), is developed to be the best benchmark of system cost analysis in this study. According to the studied hybrid solar–wind system, the annualized cost of system is composed of the annualized capital cost C_{acap}, the annualized replacement cost C_{arep} and the annualized maintenance cost C_{amain}. Five main parts are considered: PV array, wind turbine, battery, wind turbine tower and the other devices. The other devices are the equipments that are not included in the decision variables, including controller, inverter and rectifier (if it is necessary when the wind turbine is designed to have AC output). Then, the ACS can be expressed by

$$\begin{aligned}\mathrm{ACS} = {} & C_{\mathrm{acap}}(\mathrm{PV}+\mathrm{Wind}+\mathrm{Bat}+\mathrm{Tower}+\mathrm{Others}) \\ & + C_{\mathrm{arep}}(\mathrm{Bat}) + C_{\mathrm{amain}}(\mathrm{PV}+\mathrm{Wind}+\mathrm{Bat} \\ & + \mathrm{Tower}+\mathrm{Others})\end{aligned} \tag{23}$$

4.1. The annualized capital cost

The annualized capital cost of each component (PV array, wind turbine, battery, wind turbine tower and the other devices) has taken into account the installation cost (including PV array racks and cables et al.), and they are calculated by

$$C_{\mathrm{acap}} = C_{\mathrm{cap}} \cdot \mathrm{CRF}(i, Y_{\mathrm{proj}}) \tag{24}$$

where C_{cap} is the initial capital cost of each component, US$; Y_{proj} is the component lifetime, year; CRF is the capital recovery factor, a ratio to calculate the present value of an annuity (a series of equal annual cash flows). The equation for the capital recovery factor is

$$\mathrm{CRF}(i, Y_{\mathrm{proj}}) = \frac{i \cdot (1+i)^{Y_{\mathrm{proj}}}}{(1+i)^{Y_{\mathrm{proj}}} - 1} \tag{25}$$

The annual real interest rate i is related to the nominal interest rate i' (the rate at which you could get a loan) and the annual inflation rate f by the equation given below.

$$i = \frac{i' - f}{1+f} \tag{26}$$

4.2. The annualized replacement cost

The annualized replacement cost of a system component is the annualized value of all the replacement costs occurring throughout the lifetime of the project. In the studied hybrid system, only the battery needs to be replaced periodically during the project lifetime.

$$C_{\mathrm{arep}} = C_{\mathrm{rep}} \cdot \mathrm{SFF}(i, Y_{\mathrm{rep}}) \tag{27}$$

where C_{rep} is the replacement cost of the component (battery), US$; Y_{rep} is the component (battery) lifetime, year; SFF is the sinking fund factor, a ratio to calculate the future value of a series of equal annual cash flows. The equation for the sinking fund factor is

$$\mathrm{SFF}(i, Y_{\mathrm{rep}}) = \frac{i}{(1+i)^{Y_{\mathrm{rep}}} - 1} \tag{28}$$

4.3. The maintenance cost

The system maintenance cost, which has taken the inflation rate f into account, is given as

$$C_{\mathrm{amain}}(n) = C_{\mathrm{amain}}(1) \cdot (1+f)^n \tag{29}$$

where $C_{\mathrm{amain}}(n)$ is the maintenance cost of the nth year.

The initial capital cost, replacement cost, maintenance cost in the first year and the lifetime of each component (PV array, wind turbine, battery, tower and other devices) in this study are assumed as shown in Table 3.

The configuration with the lowest annualized cost of system (ACS) is taken as the optimal one from the configurations that can guarantee the required reliability of power supply.

5. System optimization model with genetic algorithm

Due to more variables and parameters that have to be considered, the sizing of the hybrid solar–wind systems is much more complicated than the single source power

Table 3
The costs and lifetime aspect for the system components

	Initial capital cost	Replacement cost	Maintenance cost in the first year	Lifetime (year)	Interest rate i' (%)	Inflation rate f (%)
PV array	6500 US$/kW	Null	65 US$/kW	25	3.75	1.5
Wind turbine	3500 US$/kW	Null	95 US$/kW	25		
Battery	1500 US$/kAh	1500 US$/kAh	50 US$/kAh	Null		
Tower	250 US$/m	Null	6.5 US$/m	25		
Other components	8000 US$	Null	80 US$	25		

generating systems. This type of optimization includes economical objectives, and it requires the assessment of long-term system performance in order to reach the best compromise for both power reliability and cost. The minimization of the cost (objective) function is implemented employing a genetic algorithm (GA), which dynamically searches for the optimal system configurations.

5.1. Genetic algorithm

A genetic algorithm (GA) is an advanced search and optimization technique. It has been developed to imitate the evolutionary principle of natural genetics. Compared with traditional methods (the direct exhaustive search method and the gradient-directed search method) for function optimization, one of the main advantages of the GA is that it is generally robust in finding global optimal solutions, particularly in multimodal and multi-objective optimization problems.

Generally, a GA uses three operators (selection, crossover and mutation) to imitate the natural evolution processes.

The first step of a genetic evaluation is to determine if the chosen system configuration (called a chromosome) passes the functional evaluation, provides service to the load within the bounds set forth by the loss of power supply probability. If the evaluation qualified chromosome has a lower annualized cost of system (ACS) than the lowest ACS value obtained at the previous iterations, this system configuration (chromosome) is considered to be the optimal solution for the minimization problem in this iteration. This optimal solution will be replaced by better solutions, if any, produced in subsequent GA generations during the program evolution.

After the selection process, the optimal solution will then be subject to the crossover and mutation operations in order to produce the next generation population until a pre-specified number of generations have been reached or when a criterion that determines the convergence is satisfied.

5.2. Methodology of the optimization model

The following optimization model is a simulation tool to obtain the optimum size or optimal configuration of a hybrid solar–wind system employing a battery bank in terms of the LPSP technique and the ACS concept by using a genetic algorithm. The flow chart of the optimization process is illustrated in Fig. 3.

The decision variables included in the optimization process are the PV module number N_{PV}, wind turbine number N_{WT}, battery number N_{bat}, PV module slope angle β' and wind turbine installation height H_{WT}. A year of hourly data including the solar radiation on the horizontal surface, ambient air temperature, wind speed and load power consumption are used in the model.

The initial assumption of system configuration will be subject to the following inequalities constraints:

$$\mathrm{Min}(N_{PV}, N_{wind}, N_{bat}) \geqslant 0 \tag{30}$$

$$H_{low} \leqslant H_{WT} \leqslant H_{high} \tag{31}$$

$$0^\circ \leqslant \beta' \leqslant 90^\circ \tag{32}$$

An initial population of 10 chromosomes, comprising the 1st generation, is generated randomly and the constraints described by inequalities (30)–(32) are evaluated for each chromosome. If any of the initial population chromosomes violates the problem constraints then it is replaced by a new chromosome, which is generated randomly and fulfils these constraints.

The PV array power output is calculated according to the PV system model by using the specifications of the PV module as well as the ambient air temperature and solar radiation conditions. The wind turbine performance calculations need to take into account the effects of wind turbine installation height. The battery bank, with total nominal capacity C'_{bat} (Ah), is permitted to discharge up to a limit defined by the maximum depth of discharge DOD, which is specified by the system designer at the beginning of the optimal sizing process.

The system configuration will then be optimized by employing a genetic algorithm, which dynamically searches for the optimal configuration to minimize the annualized cost of system (ACS). For each system configuration, the system's LPSP will be examined for whether the load requirement (LPSP target) can be satisfied. Then, the lower cost load requirement satisfied configurations, will be subject to the following crossover and mutation operations of the GA in order to produce the next generation population until a pre-specified number of generations has been reached or when a criterion that determines the convergence is satisfied.

So, for the desired LPSP value, the optimal configuration can be identified both technically and economically from the set of configurations by achieving the lowest annualized cost of system (ACS) while satisfying the LPSP requirement.

6. Results and discussion

The proposed method has been applied to analyze one hybrid project, which is designed to supply power for a telecommunication relay station on a remote island, Dalajia Island in Guangdong Province, China. A 1300 W GSM base station RBS2206 (24 V AC), and a 200 W microwave (24 V DC) are needed for the normal operation of the telecommunication station. According to the project requirements and technical considerations, a continuous power consumption of 1500 W (1300 W AC and 200 W DC) is chosen to be the hybrid system load requirement.

The technical characteristics of the PV module and battery as well as the wind turbines power curve used in the studied project are given in Tables 4 and 5 and Fig. 4. The lead-acid batteries employed in the project are specially designed for deep cyclic operation in consumer

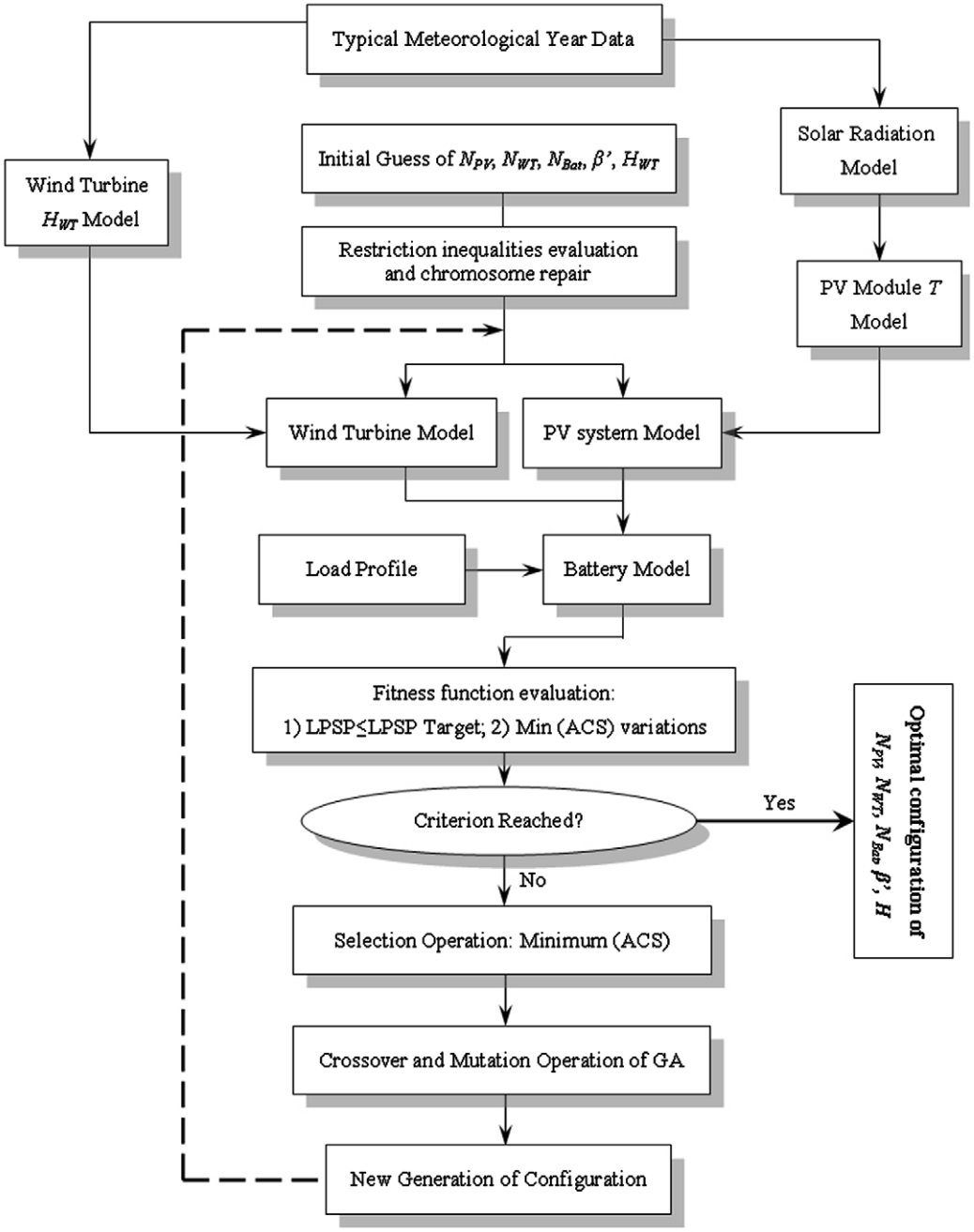

Fig. 3. Flow chart of the optimal sizing model using GA.

applications like the hybrid solar–wind systems. The manufacturer specifies a nominal capacity of 1000 Ah for each battery cell; 12 of them are connected in series to give a nominal output voltage of 24 V; these twelve battery cells are called a string. The number of strings (N_{bat}) is one of the decision variables and it will be optimized in the following process. The depth of discharge (DOD) for the battery is currently set at 80% to protect the battery from over-discharge.

The optimum combination of photovoltaic and wind energy in a hybrid system varies as the solar radiation and wind speed potentials vary during the time in question: for example, hourly, monthly, seasonally or yearly. Therefore, if the system is designed to supply electricity throughout a year, the hybrid energy system should be designed according to the yearly solar and wind resources rather than those of any other period of time.

Table 4
Specifications of the PV module

V_{oc} (V)	I_{sc} (A)	V_{max} (V)	I_{max} (A)	P_{max} (W)
21	6.5	17	5.73	100

Table 5
Specifications of the battery

Rated capacity (Ah)	Voltage (V)	Charging efficiency (%)	EFC (cycles)	Battery float life $Y_{bat,f}$ (year)
1000	24	90	560	8

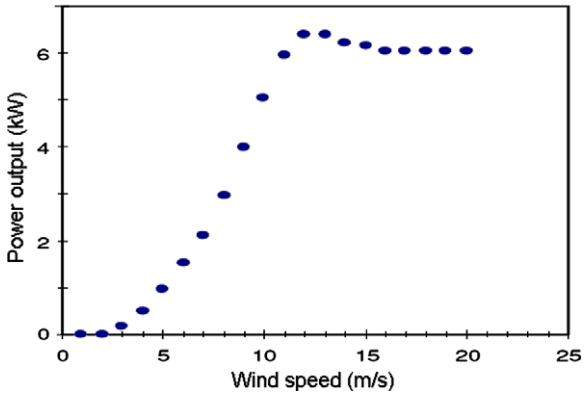

Fig. 4. Power curve of the wind turbine.

In this research, the year 1989 is chosen as the typical meteorological year (Yang and Lu, 2004) in Hong Kong to represent the climatic conditions for the studied project design in the following optimization process. The daily solar radiation on the horizontal plane, the wind speed (30 m above the ground) distribution probability as well as the hourly mean values of ambient temperature are plotted in Fig. 5. The battery temperature will vary during the changing and discharging process even if the ambient temperature remains constant, and to simplify the simulation model, the battery temperature was assumed to be constantly 5 °C higher than the ambient temperature in this study.

6.1. System optimal sizing result

Hybrid solar–wind systems usually meet load demands well because of the good complementary effect of the solar radiation and wind speed. The optimal sizing results for the LPSP of 1% and 2% are shown in Table 6, resulting in a minimum annualized cost of system of US$10,600 and US$9,708 respectively. In the following analysis, we will take LPSP = 2% as an example.

It is noteworthy that the optimized battery bank for the LPSP = 2% case turned out to have five strings of batteries, with a total nominal capacity of 5000 Ah (24 V). And the batteries in this case are well controlled in good working states with a 70.5% opportunity for its SOC remaining above 80% (see Fig. 6) for the studied typical meteorological year of 1989, and the system loss of power supply probability (LPSP) was quite well controlled to be less than 2%, as required. As a result, a reliable power supply and a long cycle lifetime of the lead-acid batteries can be ensured.

One thought-provoking phenomenon seen from the optimal sizing results is that the PV module slope angle β' is sometimes higher compared to the typical angle values calculated using the latitude of the installation site. For example, $\beta' = 24.0°$ is chosen for the case of LPSP = 2%, while the typical installation procedures usually use a slope angle of 22.5° for the site under consideration. The optimal PV module slope angle may be a little different due to different solar radiation and wind speed profiles as well as the load distributions. But generally, it is better to install the PV array at an angle higher than the local latitude to maximize power production during the low solar resource times of the year when the PV array is not supplying as much energy as in the summer period.

Also, variations of the minimum annualized cost of system during the GA optimization process are given in Fig. 7. It shows that a near optimal solution was derived during the very early stages of the GA generation evolutions.

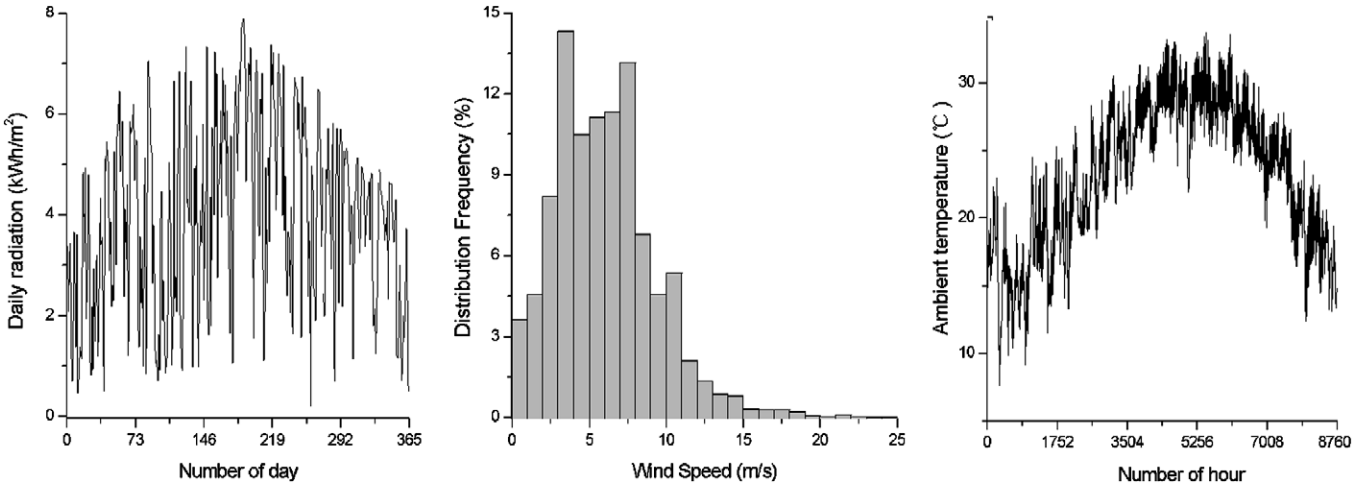

Fig. 5. Meteorological conditions for optimal design.

Table 6
Optimal sizing results for the hybrid solar–wind system for LPSP = 1% and 2%

Desired LPSP	N_{WT}	N_{PV}	N_{bat}	β' (°)	H_{WT} (m)	Cost (US$)	LPSP (%)
1%	1	128	6	24.5	31.0	10,600	0.97
2%	1	115	5	24.0	32.5	9708	1.96

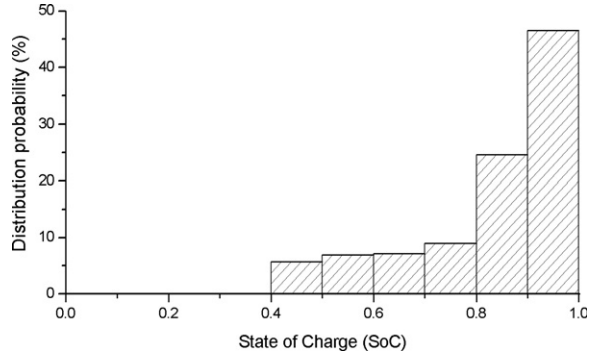

Fig. 6. Battery SOC distribution probability for optimal result.

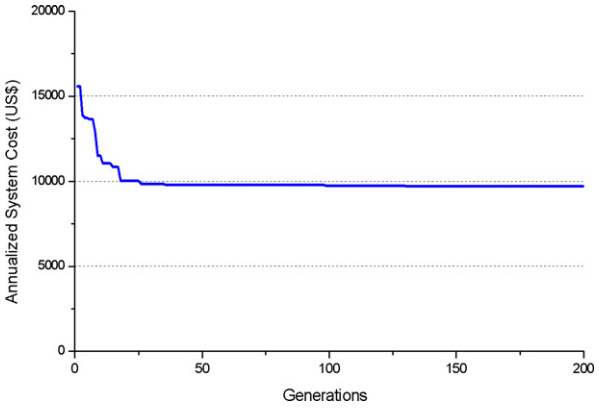

Fig. 7. Variations of ACS during GA optimization process.

The optimal sizing method can also be applied to design systems whose power source consists either only of PV modules or only of wind turbines. And the optimal sizing results for PV alone and wind turbine alone systems for the LPSP = 2% are given in Table 7. It is obvious that in both cases, the optimal configurations result in a higher annualized cost of system compared to the hybrid solar–wind system given in Table 6.

6.2. Power reliability and annualized cost of system

The minimum annualized costs of system for different LPSP (power reliability requirements) are calculated by the proposed optimal sizing method. The results for a hybrid system, PV alone system and wind turbine alone system are demonstrated in Fig. 8.

It is clear that higher power reliable systems are more expensive than lower requirement systems. Choosing an optimal system configuration according to system power reliability requirements can help save investments and avoid blind capital spending.

6.3. Power reliability and system configurations

The relationship between system power reliability and system configurations are also studied. The calculation results (PV module and wind turbine configurations under different battery capacities) for different desired power reliabilities (LPSP = 1% and 2%) are shown in the solid symbols in Figs. 9 and 10. The areas above the curves are the configurations that can ensure the required power reliability. In this study, because the load consumption is 1500 W constantly, then 1 day's battery storage equals to 1.5 strings of battery cells (1500 Ah, 24 V) based on battery nominal capacity terms.

For a desired LPSP of 1% (Fig. 9), it shows that when the battery storage is higher, the system configuration (PV module and wind turbine power) is lower. A similar situation happens to the system with an LPSP of 2% (Fig. 10), but compared to the system with an LPSP of 1%, the PV module and wind turbine power are more moderate; this shows the impact of system power reliability requirements on the system configurations.

The annualized cost of system (ACS) under different configurations was also given by the hollow symbols in Figs. 9 and 10. In the case of Fig. 9, the ACS for four and five days' battery storage are lower than the three days', but the lowest ACS point happened on the four days' line, this shows that in all likelihood the optimal value is someplace around four days' battery storage, and this is the case given in Table 6 where four days' battery storage (six strings of battery cells) has been chosen. In Fig. 10, the ACS lines at the lowest point are almost on top of each other, this would indicate that the real optimal should be somewhere in the middle between three and five days' storage, which is also constant with the optimization

Table 7
Optimal sizing results for PV alone and wind turbine alone system for LPSP = 2%

Item	N_{WT}	N_{PV}	N_{bat}	β' (°)	H_{WT} (m)	Cost (US$)	LPSP (%)
PV alone	Null	182	8	25.0	Null	11,145	1.96
Wind turbine alone	4	Null	17	Null	30.0	16,889	1.98

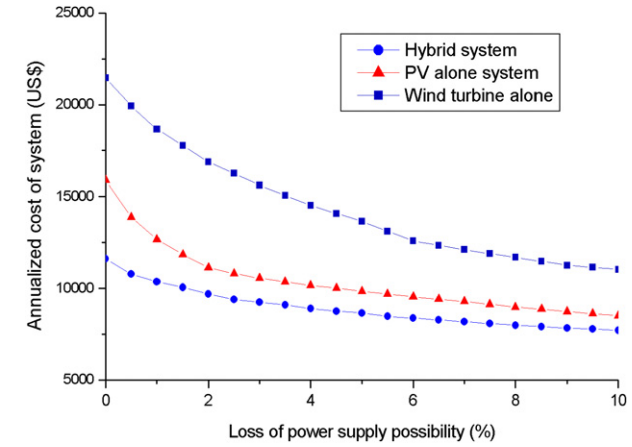

Fig. 8. ACS vs. LPSP for different systems.

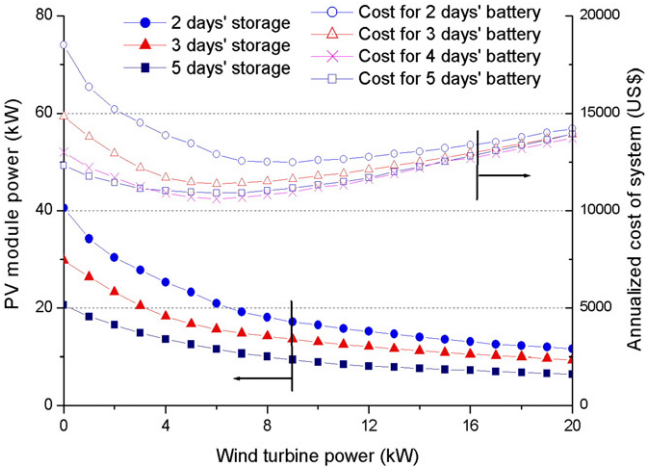

Fig. 9. System configurations and cost for LPSP = 1%.

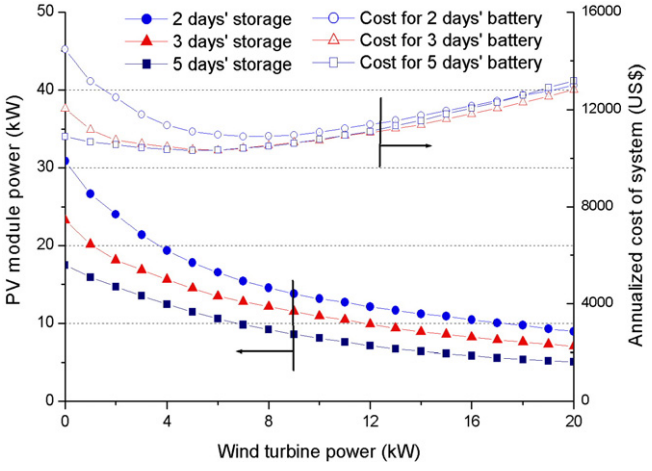

Fig. 10. System configurations and cost for LPSP = 2%.

result in Table 6 where around 3.3 days' battery storage (five strings of batteries) is selected.

Generally speaking, for the studied area, the hybrid solar–wind system with 3–5 days' battery nominal storage (batter depth-of-discharge is 80% in this study) is suitable for the desired LPSP of 1% and 2%. With the battery nominal capacity more than three times higher than the daily load energy demand, the hourly or even the daily irregular power supply from the hybrid system can be easily smoothed away. The result will change for different types of PV modules, different wind turbines, different batteries and different unit costs. The installation height of the wind turbine and PV module slope angle can also influence the simulation results.

7. Conclusions

Power supply reliability under varying weather conditions and the corresponding system cost are the two major concerns in designing PV and/or wind turbine systems. In order to utilize renewable energy resources of both solar and wind energy efficiently and economically, one optimum match design sizing method is developed in this paper based on a genetic algorithm (GA), which has the ability to attain the global optimum with relative computational simplicity compared to the conventional optimization methods. The model can be used to calculate the system optimum configuration which can achieve the desired loss of power supply probability (LPSP) with minimum annualized cost of system. The decision variables included in the optimization process are the PV module number, wind turbine number, battery number, PV module slope angle and wind turbine installation height.

The proposed method has been applied to analyze a hybrid solar–wind system to supply power for a telecommunication relay station on a remote island along the south-east coast of China. The algorithm is based upon using the weather data of year 1989 as the typical weather year for both wind speed and solar radiation for the site under consideration. Good optimal sizing performance of the algorithms has been found, and the optimal solution is a hybrid solar–wind system. Although a solar or a wind turbine only solution can also achieve the same desired LPSP, it represents a higher cost. The relationships between system power reliability and system configurations have been studied, and the hybrid system with 3–5 days' battery storage is found to be suitable for the desired LPSP of 1% and 2% for the studied case.

The loss of power supply probability (LPSP) concept used in this study is a statistical parameter. Therefore, in a bad resource year, the system will suffer from much higher probability of losing power than the desired value. System losses and other problems will also affect the system performance which would indicate that the renewable generators should be oversized to meet the actual loads in engineering practice.

References

Ashari, M., Nayar, C.V., 1999. An optimum dispatch strategy using set points for a photovoltaic (PV)–diesel–battery hybrid power system. Solar Energy 66 (1), 1–9.

Berndt, D., 1994. Maintenance-free Batteries. John Wiley & Sons, England.

Borowy, B.S., Salameh, Z.M., 1996. Methodology for optimally sizing the combination of a battery bank and PV array in a wind/PV hybrid system. IEEE Transactions on Energy Conversion 11 (2), 367–373.

Duffie, J.A., Beckman, W.A., 1980. Solar Engineering of Thermal Process. John Wiley & Sons, USA.

Eftichios, Koutroulis et al., 2006. Methodology for optimal sizing of stand-alone photovoltaic/wind-generator systems using genetic algorithms. Solar Energy 80, 1072–1188.

Gipe, Paul, 1995. Wind Energy Comes of Age. John Wiley & sons, p. 536.

Guasch, D., Silvestre, S., 2003. Dynamic battery model for photovoltaic applications. Progress in Photovoltaics: Research and Applications 11, 193–206.

Holman, J.P., 1992. Heat Transfer. McGraw-Hill.

Kellogg, W.D. et al., 1998. Generation unit sizing and cost analysis for stand-alone wind, photovoltaic and hybrid wind/PV systems. IEEE Transactions on Energy Conversion 13 (1), 70–75.

Luis, C., Sivestre, S., 2002. Modeling Photovoltaic Systems using PSpice. John Wiley & Sons Ltd, Chichester.

Markvart, T., 1996. Sizing of hybrid PV-wind energy systems. Solar Energy 59 (4), 277–281.

Perez, R., Ineichen, P., Seals, R., 1990. Modeling of daylight availability and irradiance components from direct and global irradiance. Solar Energy 44, 271–289.

Schott, T., 1985. Operational temperatures of PV modules. In: 6th PV Solar Energy Conference. pp. 392–396.

Tina, G., Gagliano, S., Raiti, S., 2006. Hybrid solar/wind power system probabilistic modeling for long-term performance assessment. Solar Energy 80, 578–588.

Van Dyk, E.E. et al., 2002. Long-term monitoring of photovoltaic devices. Renewable Energy 22, 183–197.

Yang, H.X., Burnett, L., Lu, J., 2003. Weather data and probability analysis of hybrid photovoltaic–wind power generation systems in Hong Kong. Renewable Energy 28, 1813–1824.

Yang, H.X., Lu, L., 2004. Study on typical meteorological years and their effect on building energy and renewable energy simulations. ASHRAE Transactions 110 (2), 424–431.

Yang, H.X., Lu, L., Zhou, W., 2007. A novel optimization sizing model for hybrid solar–wind power generation system. Solar Energy 81 (1), 76–84.

Zhou, W., Yang, H.X., Fang, Z.H., 2007. A novel model for photovoltaic array performance prediction. Applied Energy 84 (12), 1187–1198.